

Learnable Similarity and Dissimilarity Guided Symmetric Non-Negative Matrix Factorization

Wenlong Lyu, Yuheng Jia

Abstract—Symmetric nonnegative matrix factorization (SymNMF) is a powerful tool for clustering, which typically uses the k -nearest neighbor (k -NN) method to construct similarity matrix. However, k -NN may mislead clustering since the neighbors may belong to different clusters, and its reliability generally decreases as k grows. In this paper, we construct the similarity matrix as a weighted k -NN graph with learnable weight that reflects the reliability of each k -th NN. This approach reduces the search space of the similarity matrix learning to $n - 1$ dimension, as opposed to the $\mathcal{O}(n^2)$ dimension of existing methods, where n represents the number of samples. Moreover, to obtain a discriminative similarity matrix, we introduce a dissimilarity matrix with a dual structure of the similarity matrix, and propose a new form of orthogonality regularization with discussions on its geometric interpretation and numerical stability. An efficient alternative optimization algorithm is designed to solve the proposed model, with theoretically guarantee that the variables converge to a stationary point that satisfies the KKT conditions. The advantage of the proposed model is demonstrated by the comparison with nine state-of-the-art clustering methods on eight datasets. The code is available at <https://github.com/lwl-learning/LSDGSymNMF>.

Index Terms—Adaptive similarity, symmetric nonnegative matrix factorization, orthogonality regularization, clustering

I. INTRODUCTION

NONNEGATIVE matrix factorization (NMF) [1], [2] is a well-known dimensionality reduction method, which decomposes a non-negative data matrix $X \in \mathbb{R}_+^{m \times n}$ into two non-negative low-rank matrices $U \in \mathbb{R}_+^{m \times r}$ and $V \in \mathbb{R}_+^{n \times r}$ by solving the following problem:

$$\min_{U, V \geq 0} \|X - UV^T\|_F^2, \quad (1)$$

where m and n are the dimension and the number of data points, respectively, r is the user-specified factorization rank, and $\|X\|_F = \sqrt{\sum_{i,j} x_{ij}^2}$ is the Frobenius norm of a matrix. NMF has been successfully applied in document clustering [3], [4], facial feature extraction [1] and community detection [5]. For a comprehensive review of NMF, see [6].

Symmetric NMF (SymNMF) is a variant of NMF, which factors a pairwise similarity matrix $S \in \mathbb{R}^{n \times n}$ into the form VV^T for $V \in \mathbb{R}^{n \times r}$, i.e.,

$$\min_{V \geq 0} \|S - VV^T\|_F^2, \quad (2)$$

where r is the predefined number of clustering classes. SymNMF can be viewed as a relaxation of k -means clustering and spectral clustering [7], [8], and has the ability of clustering

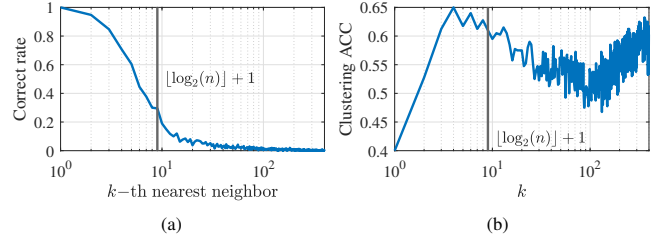


Fig. 1. (a) Correct rate of each k -th NN slice $A^{(k)}$. (b) Clustering ACC trained by standard SymNMF [7] on the ORL dataset with respect to k , where the kernel function $\kappa(x_i, x_j)$ is defined by the self-tuning method [12].

linearly non-separable data [9], [10], [11]. In SymNMF, S is usually constructed by k -nearest neighbor (k -NN) graph as follows:

$$s_{ij} = \begin{cases} \kappa(x_i, x_j), & \text{if } x_j \text{ is a } k\text{-NN of } x_i \\ 0, & \text{otherwise} \end{cases}, \quad (3)$$

where $x_i \in \mathbb{R}^m$ denotes the i -th data point, $\kappa(x_i, x_j)$ is a kernel function, e.g., $\kappa(x_i, x_j) = \exp(-\|x_i - x_j\|_2^2 / \sigma^2)$ for the Gaussian kernel. The k -NN graph S can be expressed as the sum of the first k -NN slices, i.e., $S = \sum_{i=1}^k A^{(i)}$, where the k -th NN slice $A^{(k)} \in \mathbb{R}^{n \times n}$ is defined as:

$$a_{ij}^{(k)} = \begin{cases} \kappa(x_i, x_j), & \text{if } x_j \text{ is a } k\text{-th NN of } x_i \\ 0, & \text{otherwise} \end{cases}. \quad (4)$$

Each $A^{(k)}$, $k = 1, \dots, n$ contains n neighbor relations. We name the proportion of the correct neighbor relations as the correct rate, where the correct neighbor relation means two neighboring samples x_i and x_j are with same ground-truth class.

By observing the correct rate of each $A^{(k)}$ on the ORL dataset, which is shown in Fig. 1a, we found that only the first few $A^{(k)}$ s have high ACC, and the rest contain a lot of error relations. As a result, the clustering may be misled when the parameter k in (3) is large. For example, we trained the standard SymNMF [7] on the ORL dataset, and the clustering ACC with respect to k is shown in Fig. 1b. It can be seen that the value of k has a significant impact on ACC, and high ACC usually occurs when k is small. For this reason, Luxburg [13] suggested choosing $k = \lfloor \log_2(n) \rfloor + 1$, which is widely used in SymNMF [7], [11], [14]. However, this simple strategy loses a lot of similarity information.

In this paper, we propose a more general and powerful approach to fully utilize the similarity information and reduce the impact of misleading relations on clustering, which is based on the following assumption:

Wenlong Lyu and Yuheng Jia are with the School of Computer Science and Engineering, Southeast University, Nanjing 211189, Jiangsu (email: l_w_l@seu.edu.cn; yhjia@seu.edu.cn), (Corresponding Author: Yuheng Jia)

Assumption 1: the k -th NN slice with a higher correct rate should be considered more important because they are more reliable.

To model this importance, we construct S as a weighted k -NN graph as follows:

$$S(w) = \sum_{k=1}^n w_k A^{(k)}, \quad \text{where } w \geq 0, w^T 1_n = 1. \quad (5)$$

In (5), 1_n is an n -dimensional vector full of 1s, w_k is a learnable non-negative coefficient reflecting the importance of $A^{(k)}$. The larger w_k is, the more important the k -th NN is, and $w_k = 0$ means that the k -th NN is unselected.

A similar idea was proposed in [15], which learns an adaptive k neighbors graph (not necessarily k -nearest neighbors) by exploring the local connectivity of data. Huang et. al. [16] further developed this approach in NMF, named NMFAN, whose neighbors are adaptively learned by combining local connectivity in both data and feature. Experiments have shown that this method is more competitive than k -NN [15], [16].

Another approach is to adaptively learn a better graph S from an initial low-quality graph S_0 (e.g. k -NN graph). Typically, S is assumed to have some desirable properties, which are described by some constraints or regularizations. For example, bi-stochastic structure [17], self-expressive property [18], and consistent with the available supervisory information [11], [19], [20], [21]. In this approach, the learned S heavily relies on the initial S_0 . Please see the detailed discussions in Section II-A.

A common **challenge** of the above two approaches is the high dimensionality of search space of S , i.e., n^2 , because every s_{ij} is a free variable. Even though several constrains, such as $S = S^T, \text{diag}(S) = 0, S1_n = 1_n$ can reduce the freedom of the the variables, it still remains an $\mathcal{O}(n^2)$ dimension space. Therefore, it is difficult to learn a high-quality similarity matrix in such a high dimensional space.

Differently, in our approach, we construct $S(w)$ in an $n-1$ dimensional space spanned by each $A^{(k)}, k = 1, \dots, n$. This low dimensionality makes it much easier to learn the optimal parameter w^* . Since the underlying optimal w^* is unknown, we must capture the properties that w^* has to reduce the search space. Based on the Assumption 1, w^* should consistent with the correct rate curve shown in Fig. 1a. To validate this, we test a simple model that combines (5) with (2) as follows:

$$\min_{V, w \geq 0} \frac{1}{2} \|S(w) - VV^T\|_F^2 + \frac{\mu}{2} \|S(w)\|_F^2, \quad \text{s.t. } w^T 1_n = 1, \quad (6)$$

where μ is a hyper-parameter that controls the density of $S(w)$. With proper μ , we trained (6) on the ORL dataset, the result in shown in Fig. 2. It can be seen that w^* is consistent with correct rate. More detailed results on (6) can be found in Section V-E.

To further improve the performance of (6), we assume that w^* should satisfy another property, captured by the following assumption:

Assumption 2: The ideal $S(w^*)$ should correspond to a discriminative clustering result.

In SymNMF (2) and its variant (6), the low-rank matrix V reflects the clustering result. Accordingly, VV^T can be seen

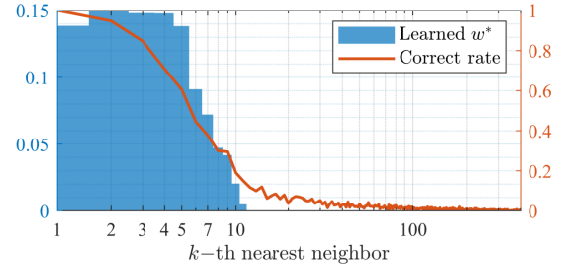


Fig. 2. The learned w^* in (6) (left y -axis) and the correct rate (right y -axis). It can be seen that w^* is sparse and consistent with correct rate.

as a similarity matrix. The larger $(VV^T)_{ij}$ is, the more likely x_i and x_j are belonging to the same class. However, as shown in Fig. 2, w^* (and $S(w^*)$) is highly sparse. Does $s_{ij}(w) = 0$ indicate that we consider x_i and x_j to be dissimilar, or we just not know their similarity? For the former, $(VV^T)_{ij}$ should be near zero; for the latter, $(VV^T)_{ij}$ should not be affected. However, the model (6) cannot distinguish between these two cases.

To address this problem, several works [22], [14] introduce a dissimilarity matrix D that with dual structure of S . When $s_{ij} = 0, d_{ij} > 0$ and $d_{ij} = 0$ can distinguish the above two cases. By simultaneously learning S and D , the discriminative of S is improved. One limitation of this approach is that additional supervision information is required to construct D .

In this paper, we notice that many of the later $A^{(k)}$ s in Fig. 2 have low correct rate, which can well reflect the dissimilarity information. Inspired by this observation, we think D can be constructed using a k -farthest neighbor graph. Similar to S , we construct D as a weighted k -NN graph with another coefficient vector $p \in \mathbb{R}^n$, i.e.:

$$D(p) = \sum_{k=1}^n p_k A^{(k)}, \quad \text{where } p \geq 0, p^T 1_n = 1. \quad (7)$$

The discriminability of clustering results is also closely related to the orthogonality of V . V can be seen as a soft clustering result, i.e., in i -th row of V , the column index corresponding to maximum element is the class index of x_i . When V is column orthogonal, i.e., $\forall i \neq j, v_i^T v_j = 0$, each row of V has only one non-zero element, which corresponds to hard clustering result. Therefore, the orthogonality constraint of V is introduced in [23]. Moreover, orthogonal NMF (ONMF) has been proven to be equivalent to weighted spherical k -means clustering [24]. Inspired by this interpretability, many ONMF methods [24], [25], [26] have been proposed to make V more discriminative. The key **challenge** in these methods is dealing with the non-convex orthogonality constraint $V^T V = I$. To this end, considering that $v_i^T v_i = 1$ is not essential, Li et. al [27] modified the constraint to a regularization $\sum_{i=1}^r \sum_{j \neq i} v_i^T v_j$. However, this formulation may lead to incorrect clustering when a column in V is all zeros, resulting the number of obtained clusters smaller than r . See the discussion in II-B for details. The negative log-determinant function can also be used as an orthogonality regularization [28], but its optimization algorithm have no theoretical guarantee of convergence.

In this paper, a new form of orthogonality regularization is proposed. By column-wisely updating, theoretical convergence is proven under the progressive hierarchical alternating least squares (PHALS) [29] framework.

The contributions of this paper are three-folds:

- 1) A new approach for similarity and dissimilarity learning is proposed, which can be seen as a weighted k -NN graph. Under this approach, the similarity relations are fully utilized, and the dimension of the search space is reduced from $\mathcal{O}(n^2)$ to $n - 1$.
- 2) A new form of orthogonality regularization is proposed, with discussions on its geometric interpretation and numerical stability. By column-wisely updating, theoretical convergence is proven under the PHALS [29] framework.
- 3) An alternative optimization algorithm is designed to solve the proposed model with $\mathcal{O}(n^2r)$ complexity per iteration. With theoretical proof, the variables converge to a stationary point that satisfied the KKT conditions.

II. RELATED WORK

A. Adaptive Similarity Methods

To adaptively learn a better graph from an initial low-quality graph, Jia et. al [18] proposed a self-expressive aware graph construction model as follows:

$$\begin{aligned} \min_{S, V \geq 0} & \|S - VV^T\|_F^2 + \alpha \|X - XS\|_F^2 + \beta \|S - S_0\|_F^2 \\ \text{s.t.,} & \text{diag}(S) = 0, \end{aligned} \quad (8)$$

where S_0 is the initial graph constructed by (3), $\text{diag}(S) = 0$ means that the diagonal elements of S are all zeros.

By leveraging ensemble clustering, S^3 NMF [30] was proposed to boost clustering performance progressively, which is formulated as:

$$\min_{S, V_i, \alpha \geq 0} \sum_{i=1}^c \alpha_i^T \|S - V_i V_i^T\|_F^2, \quad \text{s.t.,} \quad \alpha^T \mathbf{1}_n = 1, \quad (9)$$

where $V_i \in \mathbb{R}^{n \times r}$ is the i -th factor matrix, α is the weigh vector balancing the contribution of each V_i , τ is the paramater that controls the distribution of α (sharp or uniform).

Moreover, by utilizing supervisory information, Jia et. al [14] induced a dissimilarity matrix to enhance similarity learning, which is formulated as:

$$\begin{aligned} \min_{S, D, V \geq 0} & \|S - VV^T\|_F^2 + \eta \langle S, D \rangle \\ & + \alpha \text{Tr}(DL_{S_0}D^T) + \beta \text{Tr}(SL_{S_0}S^T) \\ \text{s.t.,} & s_{ij} = 1, d_{ij} = 0, \forall (i, j) \in \mathcal{M}, \\ & s_{ij} = 0, d_{ij} = 1, \forall (i, j) \in \mathcal{C}, \end{aligned} \quad (10)$$

where $L_{S_0} = \text{Diag}(S_0 \mathbf{1}_n) - S_0$ is the graph laplacian of S_0 , $\text{Diag}(x)$ is a diagonal matrix with x as its diagonal elements. \mathcal{M} and \mathcal{C} are must-link set and cannot-link set, respectively, provided by supervisory information.

In this approach, the learned S heavily relies on the initial S_0 , because S_0 either acts as the initialization of S [30] or been incorporated by a regularization like $\|S - S_0\|_F^2$ [18] and $\text{Tr}(SL_{S_0}S^T)$ [14]. Conversely, NMFAN [16] learns an

adaptive k neighbors (not necessarily k -nearest neighbors) by combining local connectivity in both data and feature spaces, which is formulated as:

$$\begin{aligned} \min_{S, U, V \geq 0} & \|X - UV^T\|_F^2 + \lambda \text{Tr}(V^T L_S V) \\ & + \mu (\text{Tr}(X^T L_S X) + \gamma \|S\|_F^2) \\ \text{s.t.,} & S^T \mathbf{1}_n = \mathbf{1}_n. \end{aligned} \quad (11)$$

A common challenge of the above methods is the $\mathcal{O}(n^2)$ dimension of search space of S , because every s_{ij} is a free variable. Therefore, it is difficult to learn a high-quality similarity matrix in such a high dimensional space. As a comparison, we construct S in an $n - 1$ dimensional space spanned by each k -th NN slice $A^{(k)}$, which makes it easier to obtain the optimal similarity in a low-dimensional space.

B. Orthogonality Regularization

The orthogonality constraint of V is introduced in [23] to enhance the discriminability of clustering result. Additionally, orthogonal NMF has been proven to be equivalent to weighted spherical k -means clustering [24]. Inspired by this interpretability, some orthogonality reglarizations are proposed to make V more discriminative. For example, the approximately orthogonal NMF [27] is formulated as

$$\begin{aligned} \min_{U, V \geq 0} & \frac{1}{2} \|X - UV^T\|_F^2 - \frac{\lambda}{2} \mathcal{R}_{\text{off-diag}}(V) \\ \text{where} & \mathcal{R}_{\text{off-diag}}(V) = -\sum_{i=1}^r \sum_{j \neq i} v_i^T v_j. \end{aligned} \quad (12)$$

The $\mathcal{R}_{\text{off-diag}}(V)$ is maximized when V is column-orthogonal, i.e., $\forall i \neq j, v_i^T v_j = 0$. Additionally, the $\mathcal{R}_{\text{off-diag}}(V)$ is also derivated in [28] by geometrically maximizing the pairwise angles between v_i and v_j . An optimization algorithm of (12) that with convergence guarantee can be seen in [31]. However, maximize $\mathcal{R}_{\text{off-diag}}(V)$ not only makes V more orthogonal, but also reduces the scale of V , which may lead to incorrect clustering when a column in V is an all-zeros vector.

Another form of orthogonality regularization is to maximize the following log-determinant function:

$$\mathcal{R}_{\log\text{-det}}(V) = \log \det(V^T V). \quad (13)$$

Geometrically, $\det(V^T V)$ is equal to the square of the volume of the parallelotope formed by the vectors $\{v_1, \dots, v_r\}$ [28]. Moreover, the $\mathcal{R}_{\log\text{-det}}(V)$ can also be written as:

$$\log \det(V^T V) = \log \prod_{i=1}^r \lambda_i(V^T V) = 2 \sum_{i=1}^r \log \sigma_i(V), \quad (14)$$

where $\lambda_i(X)$ and $\sigma_i(X)$ are the i -th largest eigenvalue and singular value of X , respectively. Once a column in V is 0_n , then $\sigma_r(V) = 0$ and $\mathcal{R}_{\log\text{-det}}(V) = +\infty$. Therefore, the disadvantage of $\mathcal{R}_{\text{off-diag}}(V)$ can be avoid. However, the optimization algorithm proposed by [28] has no theoretical guarantee of convergence.

In this paper, instead of updating V as a whole, we modified the function $\log \det(V^T V)$ into the form $v_j^T M v_j$, and updating each v_j sequentially. Due to its simplicity, the theoretical convergence is proven under the framework of progressive hierarchical alternating least squares (PHALS) [29]. This modification makes the regularization more practical and broadly applicable in NMF and SymNMF.

III. PROPOSED MODEL

A. Similarity and Dissimilarity Learning

As mentioned earlier, the similarity matrix S is usually constructed using a k -NN graph, which may mislead clustering since the NNs might belong to different clusters. Additionally, existing adaptive similarity graph learning methods suffer from the high-dimensional search space and dependence on a low-quality initial similarity matrix S_0 . To address these issues, we propose constructing S in an $n-1$ dimensional space spanned by each k -th NN slice of the affinity matrix. Specifically, let $A^{(k)} \in \mathbb{R}^{n \times n}$ represent the k -th NN slice as follows:

$$a_{ij}^{(k)} = \begin{cases} \kappa(x_i, x_j), & \text{if } x_j \text{ is a } k\text{-th NN of } x_i \\ 0, & \text{otherwise} \end{cases}. \quad (15)$$

Then, S is constructed as a weighted k -NN graph as follows:

$$S(w) = \sum_{k=1}^n w_k A^{(k)}, \quad \text{where } w \geq 0, w^T \mathbf{1}_n = 1. \quad (16)$$

In (16), $w \in \mathbb{R}^n$ is the nonnegative combination coefficient that reflects the importance of $A^{(k)}$, $k = 1, \dots, n$, and we normalize w so that $w^T \mathbf{1}_n = 1$. Due to this constraint, the dimension of w and $S(w)$ is $n-1$. Accordingly, compared with existing adaptive similarity methods that search for S in an $\mathcal{O}(n^2)$ dimensional space (as discussed in II-A), this approach is more feasible to reach the optimal similarity $S(w^*)$. Moreover, the k -NN graph S_0 defined in (3) is a special case of (16) that can be denoted as $S(w_0)$, where $w_0(1), \dots, w_0(k) = 1/k$ and $w_0(k+1), \dots, w_0(n) = 0$, i.e.:

$$\frac{1}{k} S_0 = S(w_0) = \frac{1}{k} \sum_{i=1}^k A^{(i)}. \quad (17)$$

Therefore, compared with existing methods that heavily rely on the initial S_0 , the proposed method is more stable since it leverages the entire affinity matrix by different slices $A^{(1)}, \dots, A^{(n)}$.

When k is large, $\|A^{(k)}\|_F$ becomes very small. To balance this, we normalize $A^{(k)}$ after (15) as follows:

$$\bar{A}^{(k)} \leftarrow A^{(k)} / \|A^{(k)}\|_F, \quad (18)$$

and calculate $S(w)$ in (16) using $\bar{A}^{(k)}$. In the rest of this paper, we will continue to use $A^{(k)}$ for simplicity in notation.

Based on these definitions, we propose the similarity learning model as

$$\min_{V, w \geq 0} \frac{1}{2} \|S(w) - VV^T\|_F^2 - \alpha \mathcal{R}(V), \quad \text{s.t.}, \quad w^T \mathbf{1}_n = 1. \quad (19)$$

In this model, S in (2) is replaced with $S(w)$. The term $\mathcal{R}(V)$ represents the orthogonality regularization, which will be introduced later. The hyper-parameter $\alpha \geq 0$ controls the contribution of the orthogonality regularization.

To improve the discriminative of S , we introduce a dissimilarity matrix D that with dual structure of S , which is constructed as a weighted k -NN graph with another coefficient $p \in \mathbb{R}^n$ as follows:

$$D(p) = \sum_{k=1}^n p_k A^{(k)}, \quad \text{where } p \geq 0, p^T \mathbf{1}_n = 1. \quad (20)$$

Then, the joint similarity and dissimilarity learning model is formulated as:

$$\begin{aligned} & \min_{V, w, p \geq 0} \frac{1}{2} \|S(w) - VV^T\|_F^2 + \beta \langle D(p), VV^T \rangle - \alpha \mathcal{R}(V) \\ & \text{s.t.} \quad w^T \mathbf{1}_n = p^T \mathbf{1}_n = 1, w^T p = 0, \end{aligned} \quad (21)$$

where $\langle D(p), VV^T \rangle = \sum_{i=1}^n \sum_{j=1}^n d_{ij}(p) \cdot (VV^T)_{ij}$ represents the dissimilarity regularization, $\beta \geq 0$ controls its contribution. The mechanism of the dissimilarity regularization is as follows: when $d_{ij}(p)$ is large, the x_i and x_j are considered to be dissimilar, thus the $(VV^T)_{ij}$ should be close to zero; when $d_{ij}(p)$ is near zero, the $(VV^T)_{ij}$ is unimpacted. Moreover, the constraint $w^T p = \sum_{k=1}^n w_k \cdot p_k = 0$ ensures that all $A^{(k)}$ s cannot be used to construct both similarity and dissimilarity matrices simultaneously.

Finally, our proposed model is formulated as:

$$\begin{aligned} & \min_{V, w, p \geq 0} \frac{1}{2} \|S(w) - VV^T\|_F^2 + \beta \langle D(p), VV^T \rangle - \alpha \mathcal{R}(V) \\ & \quad + \frac{\mu-1}{2} \|S(w)\|_F^2 + \frac{\mu}{2} \|D(p)\|_F^2 \\ & \text{s.t.} \quad w^T \mathbf{1}_n = p^T \mathbf{1}_n = 1, w^T p = 0, \end{aligned} \quad (22)$$

where $\frac{\mu-1}{2} \|S(w)\|_F^2$ and $\frac{\mu}{2} \|D(p)\|_F^2$ control the densities of $S(w)$ and $D(p)$, respectively. The larger the μ is, the more w_k and p_k are activated. Since the first term of (22) already includes $\frac{1}{2} \|S(w)\|_F^2$, the coefficient of the fourth term becomes $\frac{\mu-1}{2}$.

After solving (22), to get clustering result, we construct an augmented similarity matrix $Z \in \mathbb{R}^{n \times n}$ by combining the learned S, D and V . Let $Y = VV^T$, and we normalize S, D, Y into range $[0, 1]$, i.e., $S \leftarrow S / \max(S)$. Then, let

$$z_{ij} = \begin{cases} 1 - (1 - y_{ij} + d_{ij})(1 - s_{ij}), & \text{if } y_{ij} \geq d_{ij} \\ (1 + y_{ij} - d_{ij})s_{ij}, & \text{if } y_{ij} < d_{ij} \end{cases}. \quad (23)$$

When $y_{ij} \geq d_{ij}$, x_i and x_j are likely to belong to the same class, (23) will increase the corresponding similarity s_{ij} . Similarly, when $y_{ij} < d_{ij}$, s_{ij} will be depressed. Therefore, the similarity S is further enhanced. Finally, we apply spectral clustering [32] on Z to get clustering result.

B. Analysis of the Model in (22)

To better understand how our model works, we can view (22) from the perspective of V and (w, p) respectively. Before that, we first point out that $A^{(k)}$, $S(w)$ and $D(p)$ have the following useful properties:

- $\forall k, \|A^{(k)}\|_F = 1$ and $\forall k \neq t, \langle A^{(k)}, A^{(t)} \rangle = 0$;
- $\|S(w)\|_F^2 = \sum_{k=1}^n w_k^2$ and $\|D(p)\|_F^2 = \sum_{k=1}^n p_k^2$;
- $\langle S(w), D(p) \rangle = \sum_{k=1}^n w_k \cdot p_k$.

From the perspective of V , (22) is equivalent to

$$\min_{V \geq 0} \frac{1}{2} \|S(w) - \beta D(p) - VV^T\|_F^2 - \alpha \mathcal{R}(V). \quad (24)$$

When focusing on the first term, there are four cases to discuss:

- 1) $s_{ij}(w) > 0$ and $d_{ij}(p) = 0$, which means that x_i is similar to x_j , leading to $(VV^T)_{ij} > 0$
- 2) $s_{ij}(w) = 0$ and $d_{ij}(p) > 0$, which means that x_i is dissimilar to x_j , leading to $(VV^T)_{ij} \approx 0$

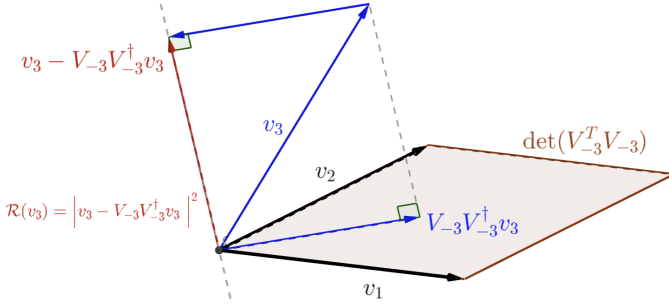


Fig. 3. The geometric meaning of $\mathcal{R}(v_3)$, which can be seen as the square of distance between v_3 and the plane spanned by $\{v_1, v_2\}$.

- 3) $s_{ij}(w) = 0$ and $d_{ij}(p) = 0$, which means that the relation between x_i and x_j is unknown. One might think that this case would lead to $(VV^T)_{ij} \approx 0$. However, VV^T is a low-rank matrix, thus the impact of this case on V is negligible compared to the second case.
- 4) $s_{ij}(w) > 0$ and $d_{ij}(p) > 0$ never occur since the constraint $w^T p = \langle S(w), D(p) \rangle = 0$.

The role of $\mathcal{R}(V)$ will be analyzed in the next subsection.

From the perspective of (w, p) , (22) is equivalent to

$$\begin{aligned} \min_{w, p \geq 0} \quad & \frac{\mu}{2} \sum_{k=1}^n (w_k^2 + p_k^2) + \sum_{k=1}^n c_k \cdot (\beta p_k - w_k) \\ \text{s.t.} \quad & w^T \mathbf{1}_n = p^T \mathbf{1}_n = 1, w^T p = 0, \end{aligned} \quad (25)$$

where $c_k = \langle A^{(k)}, VV^T \rangle$. It can be seen that μ controls the density of w and p (as well as $S(w)$ and $D(p)$, respectively), while β controls the contribution of dissimilarity regularization. Generally, the larger the k , the smaller the c_k . For example, when V is the ground-truth class assignment matrix, c_k is equivalent to the accuracy shown in Fig. 1a. This phenomenon causes w and p to automatically learn k nearest neighbors and t farthest neighbors, for some k and t , respectively, with the weights being consistent with the correct rate of $A^{(k)}$ s.

C. New Orthogonality Regularization

The role of orthogonality regularization $\mathcal{R}(V)$ is to make the learned $S(w)$ more discriminative. As discussed previously in subsection II-B, the widely used orthogonality regularization $\mathcal{R}_{\text{off-diag}}(v) = -\sum_{i=1}^r \sum_{j \neq i} v_i^T v_j$ [27] may lead to incorrect clustering when a column in V is 0_n , and $\mathcal{R}_{\log\text{-det}}(v) = \log \det(V^T V)$ [28] has no optimization algorithm that guarantees convergence. To address this problem, we modified the function $\log \det(V^T V)$ to column-wisely updating V . Specifically, the following proposition states that $\det(V^T V)$ can be reformulated into a function w.r.t. v_j .

Proposition 1. Let $V_{-j} = [v_1, \dots, v_{j-1}, v_{j+1}, \dots, v_r]$, I_n represents the identity matrix of size n , $V^\dagger \in \mathbb{R}^{r \times n}$ represents the Moore-Penrose pseudo-inverse of V . Assuming that $V \in \mathbb{R}^{n \times r}$ and $\text{rank}(V) = r$, then $\forall j = 1, \dots, r$, we have:

$$\det(V^T V) = \det(V_{-j}^T V_{-j}) v_j^T (I_n - V_{-j} V_{-j}^\dagger) v_j. \quad (26)$$

Proof. By spitting V as $V = [V_{1:j-1}, v_j, V_{j+1:r}]$, we have:

$$\begin{aligned} \det(V^T V) &= \begin{vmatrix} V_{1:j-1}^T V_{1:j-1} & V_{1:j-1}^T v_j & V_{1:j-1}^T V_{j+1:r} \\ v_j^T V_{1:j-1} & v_j^T v_j & v_j^T V_{j+1:r} \\ V_{j+1:r}^T V_{1:j-1} & V_{j+1:r}^T v_j & V_{j+1:r}^T V_{j+1:r} \end{vmatrix} \\ &= \begin{vmatrix} V_{-j}^T V_{-j} & V_{-j}^T v_j \\ v_j^T V_{-j} & v_j^T v_j \end{vmatrix}. \end{aligned} \quad (27)$$

By applying $\det \begin{pmatrix} A & B \\ C & D \end{pmatrix} = \det(D) \det(A - BD^{-1}C)$, we have:

$$\begin{vmatrix} V_{-j}^T V_{-j} & V_{-j}^T v_j \\ v_j^T V_{-j} & v_j^T v_j \end{vmatrix} = v_j^T v_j \left| V_{-j}^T V_{-j} - \frac{V_{-j}^T v_j v_j^T V_{-j}}{v_j^T v_j} \right|. \quad (28)$$

According to the Sylvester's determinant theorem: $\det(X + AB) = \det(X) \det(I_n + BX^{-1}A)$, (28) can be further simplified to

$$\begin{aligned} & (v_j^T v_j) \det(V_{-j}^T V_{-j}) \left(1 - \frac{v_j^T [V_{-j} (V_{-j}^T V_{-j})^{-1} V_{-j}^T] v_j}{v_j^T v_j} \right) \\ &= \det(V_{-j}^T V_{-j}) (v_j^T v_j - v_j^T [V_{-j} (V_{-j}^T V_{-j})^{-1} V_{-j}^T] v_j) \\ &= \det(V_{-j}^T V_{-j}) (v_j^T v_j - v_j^T [V_{-j} V_{-j}^\dagger] v_j) \\ &= \det(V_{-j}^T V_{-j}) v_j^T (I_n - V_{-j} V_{-j}^\dagger) v_j, \end{aligned} \quad (29)$$

which is the right side of (26). \square

Geometrically, $\det(V^T V)$ is equal to the square of the volume of the parallelotope formed by the vectors $\{v_1, \dots, v_r\}$ [28]. Therefore, Proposition 1 states that the $\det(V^T V)$ can be expressed as the product of $\det(V_{-j}^T V_{-j})$ and the contribution of v_j . Based on this observation, we define the orthogonality regularization w.r.t. v_j as

$$\mathcal{R}(v_j) = v_j^T (I_n - V_{-j} V_{-j}^\dagger) v_j = v_j^T M_j v_j, \quad (30)$$

where $M_j = I_n - V_{-j} V_{-j}^\dagger$. The geometric meaning of $\mathcal{R}(v_j)$ is illustrated in Fig. 3. The computational merits of $\mathcal{R}(v_j)$ are summarized as follows:

- 1) **Clustering correctness:** When maximizing $\mathcal{R}(v_j)$, v_j will not be 0_n . More generally, v_j will be far from the range space of V_{-j} , making the clustering partitions v_j be different from V_{-j} .
- 2) **Convergence guarantee:** The algorithm for solving (24) can be derived under the framework of PHALS [29] with theoretical convergence guarantee, which will be introduced in the next section.
- 3) **Numerical stability:** Since M_j is a positive semi-definite matrix whose largest eigenvalue is one, we have:

$$0 \leq \mathcal{R}(v_j) \leq \|v_j\|_2^2 \quad \text{and} \quad 0 \leq \mathcal{R}(V) \leq \|V\|_F^2. \quad (31)$$

This is much more stable than $\mathcal{R}_{\log\text{-det}}(V) = \log \det(V^T V)$, whose lower bound is $-\infty$.

Remark 1. $\mathcal{R}(V)$ cannot be explicitly expressed as a function w.r.t. V . Therefore, optimization problems with $\mathcal{R}(V)$ can only be optimized column-wisely, and V_{-j} is fixed when updating v_j .

IV. OPTIMIZATION

In this section, we propose an alternating iterative algorithm to solve (22), i.e., when updating a variable, all the other variables are fixed and treated as constants.

A. Updating V

When fixing w and p , the subproblem of (22) w.r.t. V is:

$$\min_{V \geq 0} \frac{1}{2} \|S(w) - VV^T\|_F^2 + \beta \langle D(p), VV^T \rangle - \alpha \mathcal{R}(V). \quad (32)$$

For each $j = 1, \dots, r$, V_{-j} is fixed, and the subproblem of (32) w.r.t. v_j is:

$$\min_{v_j \geq 0} \frac{1}{2} \|S(w) - V_{-j}V_{-j}^T - v_jv_j^T\|_F^2 + \beta \langle D(p), v_jv_j^T \rangle - \alpha v_j^T M_j v_j, \quad (33)$$

which can be further simplified as:

$$\min_{v_j \geq 0} \frac{1}{2} \|S(w) - \beta D(p) + \alpha M_j - V_{-j}V_{-j}^T - v_jv_j^T\|_F^2. \quad (34)$$

It can be seen that the subproblem (34) is mathematically equivalent to rank-one SymNMF, which can be efficiently solved by applying the PHALS algorithm [29].

Lemma 1 (Theorem 2, [29]). *When the PHALS algorithm is applied to solving (34), the objective functions of (34) and (32) are monotonically decreasing.*

Remark 2. *In (34), $S(w) - \beta D(p)$ is asymmetric, but it is equivalent to symmetric case because:*

$$\|M - vv^T\|_F^2 = \|\frac{M+M^T}{2} - vv^T\|_F^2 - \|\frac{M+M^T}{2}\|_F^2 + \|M\|_F^2. \quad (35)$$

B. Updating (w, p)

When fixing V , the subproblem of (22) w.r.t. (w, p) is:

$$\begin{aligned} \min_{w, p \geq 0} \frac{\mu}{2} \sum_{k=1}^n (w_k^2 + p_k^2) + \sum_{k=1}^n c_k \cdot (\beta p_k - w_k) \\ \text{s.t. } w^T \mathbf{1}_n = p^T \mathbf{1}_n = 1, w^T p = 0, \end{aligned} \quad (36)$$

where $c_k = \langle A^{(k)}, VV^T \rangle$. Mathematically, (36) is a non-convex optimization problem due to the constraint $w^T p = 0$. To solve this problem, we relax this constraint into a regularization as follows:

$$\begin{aligned} \min_{w, p \geq 0} \frac{\mu}{2} \sum_{k=1}^n (w_k^2 + p_k^2) + \sum_{k=1}^n c_k \cdot (\beta p_k - w_k) + \eta \sum_{k=1}^n w_k \cdot p_k \\ \text{s.t. } w^T \mathbf{1}_n = p^T \mathbf{1}_n = 1, \end{aligned} \quad (37)$$

where $\eta > 0$ is a hyper-parameter.

Proposition 2. *Let (w^*, p^*) be a global optimum of (37), if it satisfies:*

$$\sum_{k=1}^n w_k^* \cdot p_k^* = 0, \quad (38)$$

then (w^*, p^*) is also a global optimum of (36).

Proof. Let the objective function and the constraint space of (37) be $f(w, p, \eta)$ and $\Delta^n = \{w \in \mathbb{R}^n \mid w \geq 0, w^T \mathbf{1}_n = 1\}$,

respectively. Since (w^*, p^*) is a global optimum of (37), for any $\bar{\eta} \geq \eta$, we have:

$$f(w^*, p^*, \eta) \leq f(w, p, \eta) \leq f(w, p, \bar{\eta}), \forall w, p \in \Delta^n. \quad (39)$$

Moreover, since $\sum_{k=1}^n w_k^* \cdot p_k^* = 0$, we have $f(w^*, p^*, \eta) = f(w^*, p^*, \bar{\eta})$, which indicates that:

$$f(w^*, p^*, \bar{\eta}) \leq f(w, p, \bar{\eta}), \forall w, p \in \Delta^n. \quad (40)$$

This means that, if we replace η in (37) with $\bar{\eta}$, then (w^*, p^*) is still a global optimum. Particularly, when $\bar{\eta} = +\infty$, (37) is equivalent to (36), thus the proposition holds. \square

Proposition 2 inspires us to solve (37) instead of (36), and the following proposition provides the condition under which (37) can be efficiently solved.

Proposition 3. *If $\mu > \eta$, then (37) is $(\mu - \eta)$ -strongly convex problem, thus (37) has a unique global optimum.*

Proof. It is easy to verify that the constraint space in (37) is a convex set. Besides, the Hessian of the objective function in (37) w.r.t. (w, p) is:

$$H = \begin{bmatrix} \mu I_n & \eta I_n \\ \eta I_n & \mu I_n \end{bmatrix}. \quad (41)$$

Since $\det \begin{pmatrix} A & B \\ B & A \end{pmatrix} = \det(A - B) \det(A + B)$, the eigenvalues of H are values of λ that satisfies:

$$\det(H - \lambda I_{2n}) = (\mu - \eta - \lambda)^n (\mu + \eta - \lambda)^n = 0, \quad (42)$$

which indicates that $\lambda = \mu - \eta$ or $\lambda = \mu + \eta$. Therefore, the objective function in (37) is $(\mu - \eta)$ -strongly convex, and (37) has a unique global optimum. \square

Benefiting from the strongly convexity, (37) can be efficiently solved by alternately solving the following two subproblems at the t -th iteration:

$$w^{(t+1)} = \arg \min_{w \geq 0, w^T \mathbf{1}_n = 1} \sum_{k=1}^n \frac{\mu}{2} w_k^2 + (\eta p_k^{(t)} - c_k) \cdot w_k \quad (43a)$$

$$p^{(t+1)} = \arg \min_{p \geq 0, p^T \mathbf{1}_n = 1} \sum_{k=1}^n \frac{\mu}{2} p_k^2 + (\eta w_k^{(t+1)} + \beta c_k) \cdot p_k, \quad (43b)$$

which can be further simplified as:

$$w^{(t+1)} = \arg \min_{w \geq 0, w^T \mathbf{1}_n = 1} \|w + (\eta p^{(t)} - c)/\mu\|_2^2 \quad (44a)$$

$$p^{(t+1)} = \arg \min_{p \geq 0, p^T \mathbf{1}_n = 1} \|p + (\eta w^{(t+1)} + \beta c)/\mu\|_2^2, \quad (44b)$$

which are the simplex projection problems that can be solved exactly with $\mathcal{O}(n \log n)$ complexity [33].

By alternately solving (44a) and (44b), the (w^t, p^t) converges to the global optimum of (37) (w^*, p^*) , typically within $t_{\max} = 20$ iterations. In our experiments, the condition $\sum_{k=1}^n w_k^* \cdot p_k^* = 0$ almost always holds when $\eta = 0.99\mu$ and μ is not too large, the reason for which needs further study.

Finally, the optimization algorithm of the proposed model is summarized in Alg. 1. Instead of initializing variables randomly, we set $k_0 = \lfloor \log_2(n) \rfloor + 1$ suggested by [13]. Then, we initialize the first k_0 elements of w as $1/k_0$, and the last

$n - k_0$ elements of p as $1/(n - k_0)$, while the rest elements of w and p as zeros. V is initialized by using PHALS($S(w), V_0$) (Alg. 2, [29]), where V_0 is an $n \times r$ matrix whose elements are uniformly sampled in the range of $[0, 1]$. The stopping condition is met if any one of the following three criteria is satisfied:

- 1) The iteration count of while-loop b reaches 1000.
- 2) The relative change of loss $\frac{|\text{loss}^{(b-1)} - \text{loss}^{(b)}|}{|\text{loss}^{(b-1)}|} \leq 10^{-4}$.
- 3) The relative change of variables $\Delta_b \leq 10^{-4}$, where
$$\Delta_b = \frac{\|V^{(b)} - V^{(b-1)}\|_F}{\|V^{(b-1)}\|_F} + \frac{\|w^{(b)} - w^{(b-1)}\|_2}{\|w^{(b-1)}\|_2} + \frac{\|p^{(b)} - p^{(b-1)}\|_2}{\|p^{(b-1)}\|_2}. \quad (45)$$

C. Convergence Analysis

As mentioned previously, an advantage of the proposed orthogonality regularization is the theoretical convergence guarantee, which is described by the following two theorems.

Theorem 1. *In Alg. 1, the objective function of (22) converges to a finite value.*

Proof. In the proposed optimization algorithm, (24) and (37) are alternatively solved. For the former, one-step PHALS algorithm is applied, and the objective function of (24) is monotonically decreasing according to Lemma 1. For the latter, the global optimum is obtained. Therefore, the objective function of (22) is monotonically decreasing. Moreover, the objective function of (22) has a lower bound:

$$\begin{aligned} & \frac{1}{2} \|S(w) - VV^T\|_F^2 + \beta \langle D(p), VV^T \rangle - \alpha \mathcal{R}(V) \\ & \quad + \frac{\mu-1}{2} \|S(w)\|_F^2 + \frac{\mu}{2} \|D(p)\|_F^2 \\ & \geq \frac{1}{2} \|S(w) - VV^T\|_F^2 - \alpha \mathcal{R}(V) - \frac{1}{2} \|S(w)\|_F^2 \\ & \stackrel{(31)}{\geq} \frac{1}{2} \|S(w) - VV^T\|_F^2 - \alpha \|V\|_F^2 - \frac{1}{2} \|S(w)\|_F^2 \\ & = \frac{1}{2} \|\alpha I_n + S(w) - VV^T\|_F^2 - \alpha \text{Tr}(S(w)) \\ & \quad - \frac{\alpha^2}{2} \|I_n\|_F^2 - \frac{1}{2} \|S(w)\|_F^2 \\ & \geq -\alpha \text{Tr}(S(w)) - \frac{\alpha^2}{2} \|I_n\|_F^2 - \frac{1}{2} \|S(w)\|_F^2 \\ & = -\alpha w_1 \text{Tr}(A^{(1)}) - \frac{\alpha^2 n}{2} - \frac{1}{2} \|w\|_2^2 \\ & \geq -\sqrt{n} - \frac{\alpha^2 n}{2} - \frac{n}{2}. \end{aligned} \quad (46)$$

As a result, the objective function of (22) converges to a finite value. \square

Theorem 2. *In Alg. 1, the variable set (V, w, p) converges to a stationary point that satisfies the KKT conditions.*

Proof. Once V converges to a stationary point (i.e., $V^{(b+1)} = V^{(b)}$), (w, p) is natural a stationary point that meets the KKT conditions, since (w, p) is the global optimum of (37). Therefore, the key is to prove that each v_j converges to a stationary point that meets the KKT conditions. Denoting $M = S(w) - \beta D(p) + \alpha(I_n - V_{-j}V_{-j}^\dagger) - V_{-j}V_{-j}^T$, the KKT conditions w.r.t. v_j are:

$$\begin{cases} 2v_j v_j^T v_j - 2Mv_j - \lambda = 0 \\ v_j \geq 0, \quad \lambda \geq 0, \quad v_j \odot \lambda = 0 \end{cases}, \quad (47)$$

where λ is the Lagrange multiplier w.r.t. the constraint $v_j \geq 0$. It is easy to verify that the KKT conditions are equivalent to

$$\|v_j\|_2^2 (v_j - \max(Mv_j / \|v_j\|_2^2, 0)) = -\|v_j\|_2^2 d = 0, \quad (48)$$

Algorithm 1: Algorithm of the proposed model

Input: Slices matrix $A^{(k)} \in \mathbb{R}^{n \times n}$, $k = 1, \dots, n$,
number of classes r ,
hyper-parameters α, β, μ .

Output: V, w, p

- 1 Initialize $k_0 = \lfloor \log_2(n) \rfloor + 1$, $\eta = 0.99\mu$,
 $w = p = \text{zeros}(n, 1)$, $V_0 = \text{rand}(n, r)$.
 - 2 $w_{1:k_0} = 1/k_0$, $p_{k_0+1:n} = 1/(n - k_0)$.
 - 3 Calculate S and D by (16) and (20), respectively.
 - 4 Initialize V by using PHALS(S, V_0) (Alg. 2, [29]).
 - 5 **while** *Not convergence* **do**
 - 6 **for** $j = 1, \dots, r$ **do**
 - 7 $V_{-j} = [v_1, \dots, v_{j-1}, v_{j+1}, \dots, v_r]$.
 - 8 Calculate V_{-j}^\dagger via the reduced SVD [34].
 - 9 $M = S - \beta D + \alpha(I_n - V_{-j}V_{-j}^\dagger) - V_{-j}V_{-j}^T$
 - 10 Updating v_j by using rank-one PHALS(M, v_j).
 - 11 **for** $t = 1, \dots, 20$ **do**
 - 12 Updating w by solving (44a) (Alg. 1, [33]).
 - 13 Updating p by solving (44b) (Alg. 1, [33]).
 - 14 Calculate S and D by (16) and (20), respectively.
-

where $d = \max(Mv_j / \|v_j\|_2^2, 0) - v_j$ is an auxiliary variable in the PHALS algorithm. When $v_j = 0_n$, $d = 0_n$.

According to the Theorem 5 in [29], after a one-step updateing of v_j (i.e., line 10 in Alg. 1), the objective function of (34) $f(v_j)$ satisfies:

$$f(v_j^b) - f(v_j^{b+1}) \geq \frac{2\|v_j^b\|^4 \|d\|^2}{\|d\|^2 + 3\|d\| \cdot \|v_j^b\| + 3\|v_j^b\|^2 + \|M\|_F}, \quad (49)$$

where b is the iteration count. Moreover, Theorem 1 shows that $\lim_{b \rightarrow +\infty} f(v_j^b) - f(v_j^{b+1}) = 0$, which implies that:

$$\lim_{b \rightarrow +\infty} \|v_j^b\|^4 \|d\|^2 = 0, \quad (50)$$

i.e., the KKT condition (48). \square

D. Computational Complexity Analysis

The main complexity of Alg. 1 lies in the while-loop, which is analyzed line by line as follows:

In line 8, V_{-j}^\dagger is calculated via the reduced SVD [34], which requires $\mathcal{O}(n(r-1)^2)$ complexity.

From line 9 to line 10, the PHALS algorithm does not use M directly, but only needs to calculate Mv_j , i.e.,

$$Mv_j = (S - \beta D)v_j + \alpha v_j - V_{-j} \left[\left(\alpha V_{-j}^\dagger + V_{-j}^T \right) v_j \right], \quad (51)$$

which requires only $\mathcal{O}(n^2 + n(r-1))$ complexity. Therefore, the complexity from line 6 to line 10 is $\mathcal{O}(n^2 r + nr^2)$.

According to [33], the complexities of line 12 and line 13 are $\mathcal{O}(n \log n)$.

In line 14, (16) and (20) involve the summation of n $\mathbb{R}^{n \times n}$ matrices. However, each $A^{(k)}$ is a sparse matrix with only n non-zero elements. Due to this sparsity, (16) and (20) require only $\mathcal{O}(n^2)$ computational complexity.

In summary, each iteration's complexity of the proposed algorithm is $\mathcal{O}(n^2 r + nr^2 + n \log n)$.

TABLE I
DETAILS OF DATASETS

Dataset	Dimension	# Sample (n)	# Cluster (r)
SEEDS	7	210	3
YaleB	32×32	165	15
ORL	32×32	400	40
CHART	60	600	6
USPS-1000	16×16	1000	10
COIL20	32×32	1440	20
NIST-2000	28×28	2000	10
Semeion	16×16	1593	10

V. EXPERIMENT

A. Experiment Settings

We compared the proposed method with five fixed similarity based methods: SymNMF [7], [10], ANLS [35], sBSUM [36], PHALS [29], GSNMF [37]; and four state-of-the-art adaptive similarity based methods: NMFAN [16], CGSymNMF [18], RBSMF [17], S^3 NMF [30]. For all methods, we adopted the same initial V and k -NN graph S_0 , where elements in V were uniformly sampled in the range of $[0, 1]$, and S_0 was constructed according to (3) with $k = \lfloor \log_2(n) \rfloor + 1$ as suggested by [13] and the kernel function $\kappa(x_i, x_j)$ defined by the self-tuning method [12]. To generate the clustering result of the proposed model, we performed the spectral clustering method [32] on the augmented similarity matrix Z (defined in (23)) 20 times, and reported the average performance.

For fair comparison, the hyper-parameters of ANLS, NMFAN, CGSymNMF, RBSMF and S^3 NMF were exhaustively searched in the grid provided in the original papers. For GSNMF and GSNMF, hyper-parameters were tuned in the range of $\text{logspace}(-2, 4, 50)$, i.e., 50 numbers spaced evenly on a log scale from 10^{-2} to 10^4 . For SymNMF, PHALS and sBSUM, there are no hyper-parameters to tune. For the proposed model, α , β and μ were tuned in the range of $\{0.01, 0.03, 0.07, 0.1, 0.3, 0.7, 1\}$, $\{1, 5, 10, 50, 100, 500, 1000\}$ and $\{0.05, 0.07, 0.1, 0.3, 0.5, 0.7, 1\}$, respectively. Then, we reported their average performance and the associated standard deviation (std) of 20 repetitions. We evaluated all the methods on eight commonly used datasets. The detailed information about these datasets is summarized in Table I.

We adopted two commonly used metrics, namely clustering accuracy (ACC) and normalized mutual information (NMI), to evaluate all the methods. Both values of ACC and NMI lie in the range of $[0, 1]$, and the larger, the better.

B. Comparisons of Clustering Performance

Table II shows the clustering performance of all the methods on each dataset, where the best performance under each metric is marked by bold, and the second best is underlined. From Table II, we can observe that:

- Our method significantly outperforms the compared methods, achieving the highest ACC/NMI values in most cases (13/16) and the second highest in the rest (3/16).
- The adaptive similarity methods outperforms the fixed similarity methods. There is only one case where a fixed

similarity method achieves the second-best performance: the ACC of PHALS on the YaleB dataset.

- Among the compared methods, RBSMF and S^3 NMF have good performance. The reasons may be as follows: In RBSMF, the similarity matrix is assumed to have a bi-stochastic structure, making it easier to learn a high-quality similarity matrix. Moreover, it adopts a robust loss function instead of the Frobenius norm in NMF to handle outliers. In S^3 NMF, the similarity matrix is iteratively boosted according to multiple clustering results, making it more robust to handle poor initial similarity matrix.

C. Learned Coefficients of w and p

The correct rate and the learned w and p of each dataset are shown in Fig. 4. Generally, as k increases, correct rate decreases. This phenomenon causes w and p automatically learn k nearest neighbors and t farthest neighbors, for some k and t , respectively, with the weights being consistent with the correct rate. That is, the larger the correct rate, the larger the w and the smaller the p . Moreover, w and p have no overlap, indicating that the condition in (38) is satisfied, i.e., the non-convex problem (36) can be solved equivalently by the strongly convex problem (37).

D. Hyper-parameters Analysis

There are three hyper-parameters α , β and μ in the proposed model, which control the contributions of the orthogonality regularization, the dissimilarity regularization, and the density regularization, respectively. In this subsection, we investigate their influence on the ACC of the proposed model in Fig. 5, we can be observed that:

- A larger β usually leads to higher ACCs, but at the same time, lower α often results in inferior ACCs. This is because when $\beta \langle D(p), VV^T \rangle$ is dominant, it becomes easy to learn a V of all zeros. However, when α is large, $\|V\|_F^2$ is maximized, which helps avoid this undesirable solution.
- Taking into account the ACC of all datasets, we suggest $\mu = \alpha = 0.1, \beta = 10$ as default setting.

E. Ablation Study

In this subsection, we evaluated the importance of different components of the proposed model. Specifically, we remove the orthogonality regularization and the dissimilarity matrix $D(p)$ from the proposed model (22), as shown in (52) and (53), respectively, and remove them both as shown in (54).

$$\begin{aligned} \min_{V, w, p \geq 0} & \frac{1}{2} \|S(w) - VV^T\|_F^2 + \beta \langle D(p), VV^T \rangle \\ & + \frac{\mu-1}{2} \|S(w)\|_F^2 + \frac{\mu}{2} \|D(p)\|_F^2 \quad (52) \\ \text{s.t.} & \quad w^T \mathbf{1}_n = p^T \mathbf{1}_n = 1, w^T p = 0, \end{aligned}$$

$$\begin{aligned} \min_{V, w \geq 0} & \frac{1}{2} \|S(w) - VV^T\|_F^2 - \alpha \mathcal{R}(V) + \frac{\mu}{2} \|S(w)\|_F^2 \quad (53) \\ \text{s.t.} & \quad w^T \mathbf{1}_n = 1, \end{aligned}$$

$$\min_{V, w \geq 0} \frac{1}{2} \|S(w) - VV^T\|_F^2 + \frac{\mu}{2} \|S(w)\|_F^2 \quad \text{s.t.} \quad w^T \mathbf{1}_n = 1. \quad (54)$$

TABLE II
CLUSTERING PERFORMANCE ON EACH DATASET.

ACC	SEEDS	YaleB	ORL	CHART	USPS-1000	COIL20	MNIST-2000	Semeion
SymNMF	0.658 ± 0.126	0.458 ± 0.018	0.616 ± 0.022	0.632 ± 0.059	0.514 ± 0.041	0.503 ± 0.038	0.535 ± 0.042	0.547 ± 0.066
ANLS	0.753 ± 0.132	0.459 ± 0.017	0.614 ± 0.013	0.643 ± 0.056	0.531 ± 0.044	0.557 ± 0.037	0.567 ± 0.053	0.576 ± 0.052
sBSUM	0.840 ± 0.029	0.461 ± 0.013	0.620 ± 0.014	0.595 ± 0.057	0.562 ± 0.047	0.644 ± 0.066	0.565 ± 0.067	0.615 ± 0.060
PHALS	0.789 ± 0.120	0.467 ± 0.015	0.621 ± 0.015	0.646 ± 0.062	0.532 ± 0.041	0.658 ± 0.043	0.603 ± 0.051	0.594 ± 0.043
GSNMF	0.647 ± 0.092	0.455 ± 0.024	0.620 ± 0.017	0.647 ± 0.087	0.498 ± 0.050	0.504 ± 0.034	0.493 ± 0.043	0.495 ± 0.038
NMFAN [‡]	0.876 ± 0.008	0.450 ± 0.017	0.678 ± 0.007	0.627 ± 0.075	0.463 ± 0.029	0.660 ± 0.016	0.516 ± 0.044	0.611 ± 0.044
CGSymNMF [‡]	0.755 ± 0.109	0.459 ± 0.032	0.621 ± 0.025	0.661 ± 0.080	0.487 ± 0.042	0.591 ± 0.048	0.506 ± 0.042	0.480 ± 0.037
RBSMF [‡]	0.897 ± 0.012	0.462 ± 0.014	0.645 ± 0.007	0.568 ± 0.000	0.571 ± 0.002	0.800 ± 0.000	0.665 ± 0.011	0.637 ± 0.041
S ³ NMF [‡]	0.835 ± 0.041	0.450 ± 0.008	0.617 ± 0.007	0.829 ± 0.016	0.650 ± 0.021	0.781 ± 0.015	0.664 ± 0.020	0.704 ± 0.017
proposed [‡]	0.887 ± 0.016	0.539 ± 0.020	0.683 ± 0.014	0.733 ± 0.057	0.610 ± 0.027	0.833 ± 0.015	0.698 ± 0.023	0.734 ± 0.055

NMI	SEEDS	YaleB	ORL	CHART	USPS-1000	COIL20	MNIST-2000	Semeion
SymNMF	0.400 ± 0.147	0.522 ± 0.017	0.789 ± 0.010	0.710 ± 0.066	0.529 ± 0.030	0.689 ± 0.021	0.523 ± 0.026	0.553 ± 0.043
ANLS	0.551 ± 0.143	0.526 ± 0.012	0.787 ± 0.007	0.767 ± 0.041	0.553 ± 0.028	0.743 ± 0.027	0.562 ± 0.042	0.585 ± 0.036
sBSUM	0.646 ± 0.029	0.527 ± 0.009	0.791 ± 0.007	0.784 ± 0.040	0.578 ± 0.030	0.833 ± 0.026	0.620 ± 0.041	0.632 ± 0.026
PHALS	0.580 ± 0.141	0.530 ± 0.008	0.789 ± 0.007	0.790 ± 0.028	0.568 ± 0.023	0.819 ± 0.024	0.613 ± 0.036	0.617 ± 0.022
GSNMF	0.392 ± 0.091	0.522 ± 0.017	0.786 ± 0.009	0.714 ± 0.053	0.508 ± 0.042	0.678 ± 0.025	0.423 ± 0.041	0.488 ± 0.030
NMFAN [‡]	0.642 ± 0.014	0.501 ± 0.014	0.830 ± 0.006	0.626 ± 0.025	0.445 ± 0.037	0.756 ± 0.017	0.457 ± 0.027	0.554 ± 0.031
CGSymNMF [‡]	0.548 ± 0.096	0.522 ± 0.021	0.800 ± 0.013	0.704 ± 0.065	0.495 ± 0.041	0.769 ± 0.031	0.501 ± 0.036	0.465 ± 0.035
RBSMF [‡]	0.687 ± 0.021	0.534 ± 0.003	0.806 ± 0.004	0.801 ± 0.001	0.627 ± 0.002	0.892 ± 0.000	0.654 ± 0.008	0.649 ± 0.016
S ³ NMF [‡]	0.647 ± 0.055	0.512 ± 0.006	0.787 ± 0.004	0.809 ± 0.017	0.625 ± 0.016	0.860 ± 0.007	0.636 ± 0.015	0.665 ± 0.011
proposed [‡]	0.709 ± 0.021	0.586 ± 0.012	0.846 ± 0.006	0.809 ± 0.011	0.627 ± 0.015	0.923 ± 0.012	0.691 ± 0.011	0.678 ± 0.021

[‡]: Adaptive similarity methods.

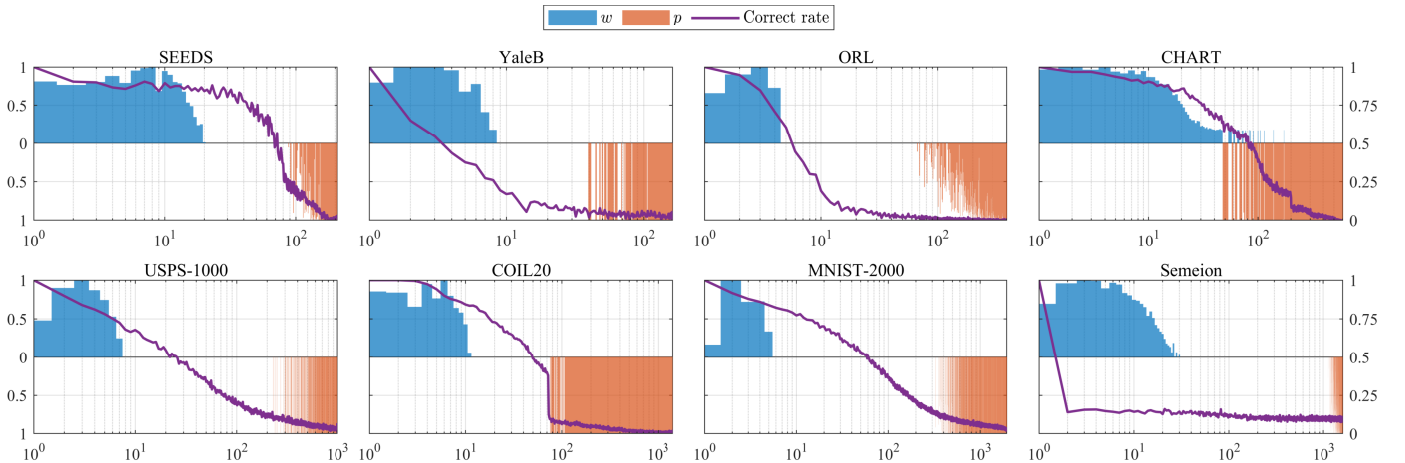


Fig. 4. Correct rate and the learned w and p of each dataset. The x -axis represents the k -th nearest neighbors on a logarithmic scale. The upper and lower parts of the left y -axis represents the coordinates of w and p respectively, and the right y -axis is the coordinate of correct rate. For better view, w and p are normalized to the range $[0, 1]$.

For a fair comparison, the hyperparameters of (52), (53) and (54) were carefully tuned on a larger and more dense grid. Specifically, for (52), μ was tuned in the range of $\{0.03, 0.05, 0.07, 0.1, 0.3, 0.5, 0.7, 1, 1.2\}$, and β was tuned in the range of $\{1, 5, 10, 30, 70, 100, 300, 700, 1000\}$; in (53), μ and α were tuned in the range of $\{0.1, 0.3, 0.5, 0.7, 1, 3, 5, 7, 10\}$; in (54), μ was tuned in the range of $\text{logspace}(-2, 2, 50)$.

The clustering performances of these models are shown in Table III. Comparing the results of (52) and (54) as well as (22) and (53), it can be seen that the dissimilarity matrix can improve the clustering performance. Similarly, comparing the results of (53) and (54) as well as (22) and (52), it can be seen that the proposed orthogonality regularization can significantly improve the clustering performance. These two

improvements are especially evident on the COIL20, MNIST-2000 and Semeion datasets. It may be because the number of samples n in these datasets is relatively large, making it difficult to search for high-quality S in an n -dimensional space. By introducing D and enhancing the orthogonality regularization of V , the discriminative ability of S is improved, which makes S easier to learn.

F. Advantage of the proposed orthogonality regularization

In this subsection, we analyzed the advantage of the proposed orthogonality regularization $\mathcal{R}(V)$ compared with the aforementioned $\mathcal{R}_{\text{off-diag}} = -\sum_{i=1}^r \sum_{j \neq i} v_i^T v_j$ [27] and $\mathcal{R}_{\text{log-det}} = \log \det(V^T V)$ [28]. After replacing $\mathcal{R}(V)$ in (22) with $\mathcal{R}_{\text{off-diag}}$ and $\mathcal{R}_{\text{log-det}}$, multiplicative update (MU)

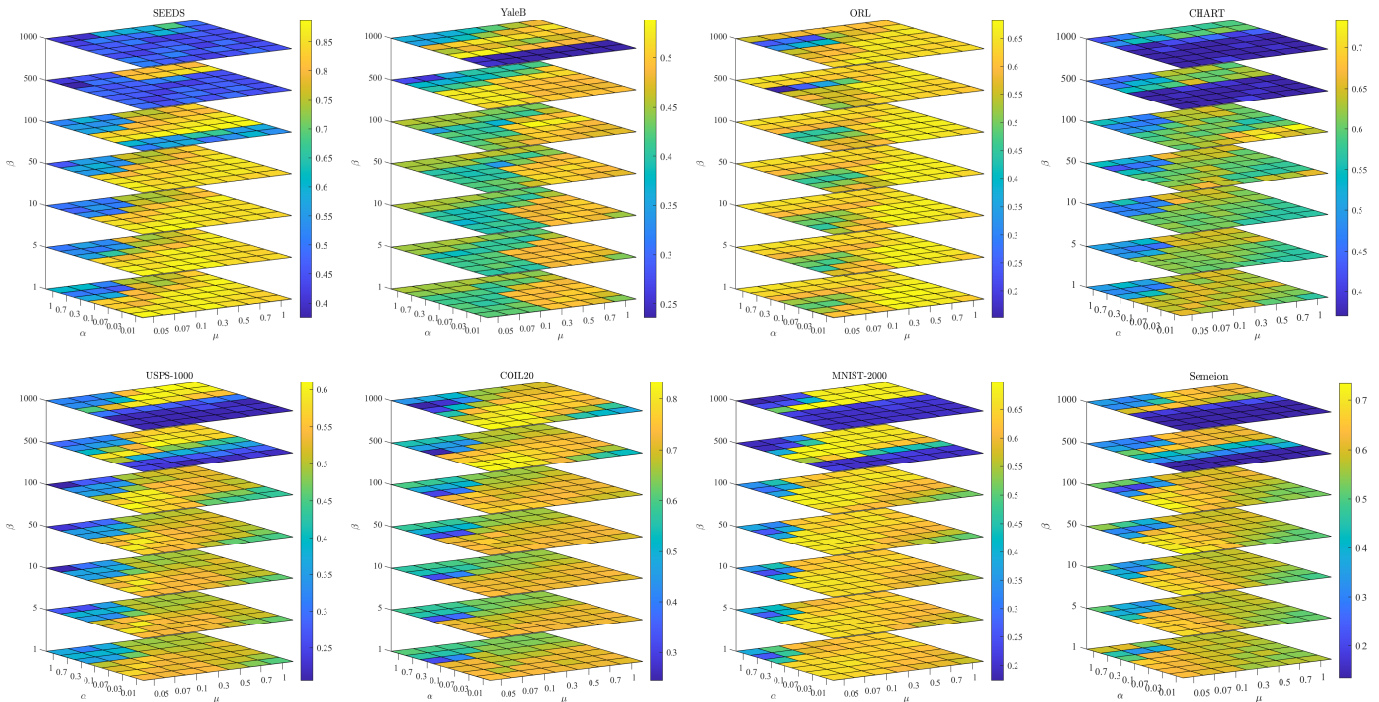


Fig. 5. Average values of ACC of the proposed model with different values of α , β and μ . They are all 4-D figures, where the fourth direction is indicated by the color with the corresponding color bar.

TABLE III
ABLATION STUDY OF THE PROPOSED MODEL.

D	Orth	SEEDS	YaleB	ORL	CHART	USPS-1000	COIL20	MNIST-2000	Semeion
(54)		0.790 \pm 0.071	0.513 \pm 0.007	0.668 \pm 0.010	0.864 \pm 0.023	0.412 \pm 0.018	0.560 \pm 0.037	0.487 \pm 0.003	0.536 \pm 0.019
(52)	✓	0.896 \pm 0.021	0.492 \pm 0.016	0.635 \pm 0.005	0.672 \pm 0.093	0.502 \pm 0.040	0.749 \pm 0.037	0.657 \pm 0.044	0.601 \pm 0.035
(53)	✓	0.878 \pm 0.030	<u>0.518 \pm 0.022</u>	<u>0.672 \pm 0.010</u>	0.686 \pm 0.115	<u>0.608 \pm 0.020</u>	<u>0.784 \pm 0.051</u>	0.661 \pm 0.038	0.760 \pm 0.033
(22)	✓	<u>0.887 \pm 0.016</u>	0.539 \pm 0.020	0.683 \pm 0.014	<u>0.733 \pm 0.057</u>	0.610 \pm 0.027	0.833 \pm 0.015	0.698 \pm 0.023	<u>0.734 \pm 0.055</u>
D	Orth	SEEDS	YaleB	ORL	CHART	USPS-1000	COIL20	MNIST-2000	Semeion
(54)		0.545 \pm 0.090	0.554 \pm 0.061	0.798 \pm 0.002	0.824 \pm 0.019	0.386 \pm 0.013	0.727 \pm 0.030	0.441 \pm 0.007	0.493 \pm 0.019
(52)	✓	0.722 \pm 0.028	0.544 \pm 0.015	0.830 \pm 0.005	0.807 \pm 0.012	0.531 \pm 0.032	0.887 \pm 0.017	0.623 \pm 0.030	0.621 \pm 0.021
(53)	✓	0.695 \pm 0.035	<u>0.575 \pm 0.013</u>	<u>0.832 \pm 0.005</u>	0.800 \pm 0.007	<u>0.618 \pm 0.022</u>	<u>0.888 \pm 0.023</u>	<u>0.658 \pm 0.015</u>	0.682 \pm 0.015
(22)	✓	<u>0.709 \pm 0.021</u>	0.586 \pm 0.012	0.846 \pm 0.006	0.809 \pm 0.011	0.627 \pm 0.015	0.923 \pm 0.012	0.691 \pm 0.011	0.678 \pm 0.021

algorithm is applied to solve the models. As a controlled experiment, we also apply MU to solve (22) using our proposed regularization. Moreover, the model (52) without orthogonality regularization is used as a blank control reference.

The clustering performances of these models are shown in Table IV. Surprisingly, the performances of the MU-based methods are worse than model (52) without orthogonality regularization. This is because MU-based methods are more sensitive to the initializations, as reflected in their larger std. Nevertheless, benefiting from the effectiveness of the PHALS algorithm, the performance of the proposed $\mathcal{R}(V)$ achieves the best performance. Moreover, among the MU-based methods, the proposed $\mathcal{R}(V)$ has a slight advantage.

Furthermore, the proposed orthogonality regularization can be applied in both NMF and SymNMF. As an example, we propose a toy model named approximately orthogonal

SymNMF (AOSymNMF) as follows:

$$\min_{V \geq 0} \frac{1}{2} \|S - VV^T\|_F^2 - \alpha \mathcal{R}(V). \quad (55)$$

Similarly, we replaced $\mathcal{R}(V)$ in (55) with $\mathcal{R}_{\text{off-diag}}$ and $\mathcal{R}_{\text{log-det}}$ and applied MU to solve them. As a controlled experiment, we also applied MU to solve (55) using our proposed regularization. Additionally, we use SymNMF and PHALS as blank control references. The hyper-parameter α in AOSymNMF is exhaustively searched in $\text{logspace}(-2, 4, 50)$.

The clustering performances of these models are shown in Table V. It can be seen that orthogonality regularization can significantly improve the clustering performance. Among the MU-based methods, the proposed $\mathcal{R}(V)$ has a slight advantage compared with $\mathcal{R}_{\text{off-diag}}(V)$ and $\mathcal{R}_{\text{log-det}}(V)$. Benefiting from the effectiveness of the PHALS algorithm, the performance of the proposed $\mathcal{R}(V)$ is further improved. As a result, the

TABLE IV
CLUSTERING PERFORMANCE OF THE PROPOSED MODEL WITH DIFFERENT $\mathcal{R}(V)$.

ACC	SEEDS	YaleB	ORL	CHART	USPS-1000	COIL20	MNIST-2000	Semeion
Model (52)	0.878 ± 0.030	0.518 ± 0.022	0.672 ± 0.010	0.686 ± 0.115	0.608 ± 0.020	0.784 ± 0.051	0.661 ± 0.038	0.760 ± 0.033
$\mathcal{R}_{\text{off-diag}}(V)$	0.853 ± 0.054	0.500 ± 0.013	0.666 ± 0.015	0.662 ± 0.069	0.517 ± 0.041	0.715 ± 0.022	0.656 ± 0.037	0.591 ± 0.066
$\mathcal{R}_{\text{log-det}}(V)$	0.846 ± 0.072	0.498 ± 0.011	0.652 ± 0.016	0.661 ± 0.070	0.565 ± 0.038	0.711 ± 0.050	0.678 ± 0.031	0.625 ± 0.068
$\mathcal{R}(V)$ by MU	0.870 ± 0.017	0.490 ± 0.016	0.672 ± 0.015	0.661 ± 0.070	0.569 ± 0.034	0.718 ± 0.018	0.679 ± 0.029	0.640 ± 0.065
Proposed $\mathcal{R}(V)$	0.887 ± 0.016	0.539 ± 0.020	0.683 ± 0.014	0.733 ± 0.057	0.610 ± 0.027	0.833 ± 0.015	0.698 ± 0.023	0.734 ± 0.055

NMI	SEEDS	YaleB	ORL	CHART	USPS-1000	COIL20	MNIST-2000	Semeion
Model (52)	0.722 ± 0.028	0.544 ± 0.015	0.830 ± 0.005	0.807 ± 0.012	0.531 ± 0.032	0.887 ± 0.017	0.623 ± 0.030	0.621 ± 0.021
$\mathcal{R}_{\text{off-diag}}(V)$	0.654 ± 0.083	0.555 ± 0.010	0.830 ± 0.007	0.799 ± 0.015	0.542 ± 0.022	0.831 ± 0.027	0.645 ± 0.025	0.604 ± 0.040
$\mathcal{R}_{\text{log-det}}(V)$	0.632 ± 0.106	0.552 ± 0.009	0.829 ± 0.008	0.800 ± 0.021	0.581 ± 0.027	0.833 ± 0.027	0.660 ± 0.024	0.623 ± 0.035
(22) by MU	0.672 ± 0.026	0.552 ± 0.011	0.832 ± 0.007	0.802 ± 0.019	0.589 ± 0.022	0.833 ± 0.026	0.666 ± 0.025	0.631 ± 0.035
Proposed $\mathcal{R}(V)$	0.709 ± 0.021	0.586 ± 0.012	0.846 ± 0.006	0.809 ± 0.011	0.627 ± 0.015	0.923 ± 0.012	0.691 ± 0.011	0.678 ± 0.021

TABLE V
CLUSTERING PERFORMANCE OF THE AOSymNMF (55) WITH DIFFERENT $\mathcal{R}(V)$.

ACC	SEEDS	YaleB	ORL	CHART	USPS-1000	COIL20	MNIST-2000	Semeion
SymNMF	0.658 ± 0.126	0.458 ± 0.018	0.616 ± 0.022	0.632 ± 0.059	0.514 ± 0.041	0.503 ± 0.038	0.535 ± 0.042	0.547 ± 0.066
PHALS	0.753 ± 0.132	0.459 ± 0.017	0.614 ± 0.013	0.643 ± 0.056	0.531 ± 0.044	0.557 ± 0.037	0.567 ± 0.053	0.576 ± 0.052
$\mathcal{R}_{\text{off-diag}}(V)$	0.672 ± 0.115	0.463 ± 0.022	0.619 ± 0.011	0.634 ± 0.075	0.537 ± 0.049	0.512 ± 0.038	0.549 ± 0.046	0.550 ± 0.054
$\mathcal{R}_{\text{log-det}}(V)$	0.722 ± 0.114	0.462 ± 0.021	0.628 ± 0.024	0.620 ± 0.046	0.534 ± 0.050	0.549 ± 0.027	0.563 ± 0.066	0.573 ± 0.055
$\mathcal{R}(V)$ by MU	0.800 ± 0.077	0.462 ± 0.018	0.626 ± 0.023	0.615 ± 0.092	0.541 ± 0.047	0.562 ± 0.035	0.592 ± 0.049	0.587 ± 0.058
Proposed $\mathcal{R}(V)$	0.835 ± 0.068	0.468 ± 0.017	0.630 ± 0.018	0.634 ± 0.089	0.568 ± 0.030	0.717 ± 0.052	0.640 ± 0.047	0.623 ± 0.053

NMI	SEEDS	YaleB	ORL	CHART	USPS-1000	COIL20	MNIST-2000	Semeion
SymNMF	0.400 ± 0.147	0.522 ± 0.017	0.789 ± 0.010	0.710 ± 0.066	0.529 ± 0.030	0.689 ± 0.021	0.523 ± 0.026	0.553 ± 0.043
PHALS	0.551 ± 0.143	0.526 ± 0.012	0.787 ± 0.007	0.767 ± 0.041	0.553 ± 0.028	0.743 ± 0.027	0.562 ± 0.042	0.585 ± 0.036
$\mathcal{R}_{\text{off-diag}}(V)$	0.429 ± 0.114	0.535 ± 0.011	0.787 ± 0.006	0.714 ± 0.048	0.549 ± 0.038	0.695 ± 0.024	0.541 ± 0.040	0.541 ± 0.035
$\mathcal{R}_{\text{log-det}}(V)$	0.498 ± 0.124	0.529 ± 0.012	0.793 ± 0.010	0.725 ± 0.058	0.552 ± 0.036	0.725 ± 0.018	0.556 ± 0.040	0.580 ± 0.043
$\mathcal{R}(V)$ by MU	0.557 ± 0.094	0.527 ± 0.013	0.791 ± 0.012	0.711 ± 0.064	0.560 ± 0.026	0.739 ± 0.018	0.568 ± 0.038	0.588 ± 0.027
Proposed $\mathcal{R}(V)$	0.634 ± 0.068	0.532 ± 0.017	0.796 ± 0.009	0.784 ± 0.033	0.593 ± 0.030	0.868 ± 0.017	0.656 ± 0.029	0.637 ± 0.022

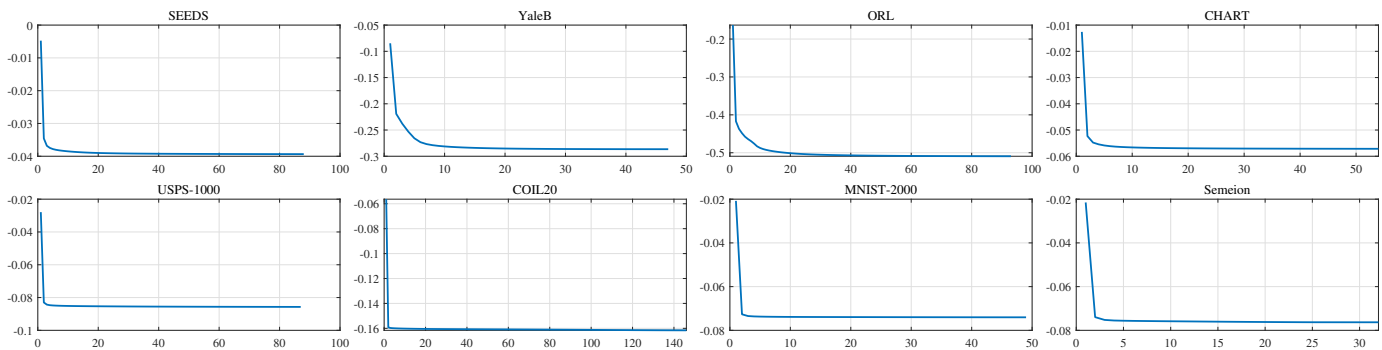


Fig. 6. Convergence curves of the proposed model (22) on eight datasets. For each dataset, the x -axis represents the iteration count, and the y -axis represents the objective function of (22).

proposed $\mathcal{R}(V)$ demonstrates significant advantages among all methods.

G. Convergence Analysis

The theoretical convergence guarantee is a key advantage of our proposed orthogonality regularization, as analyzed in Theorem 1 and Theorem 2. In this subsection, we empirically verify the empirical convergence behavior in Fig. 6, where the hyperparameters $\mu = \alpha = 0.1, \beta = 10$. It can be found that the objective function is monotonically decreases, and typically converges within 100 iterations.

VI. CONCLUSION

In this paper, we proposed a novel SymNMF model that constructs the similarity graph and dissimilarity graph as weighted k -NN graph, and adaptively learns the weights and clustering results simultaneously. Moreover, a new orthogonality regularization with explicit geometric meaning and good numerical stability is proposed. The proposed model is solved by an alternative optimization algorithm with theoretical convergence guarantee. Extensive experimental results demonstrate that the proposed model can achieve excellent clustering performance.

REFERENCES

- [1] D. Lee and H. Seung, "Learning the parts of objects by non-negative matrix factorization," *Nature*, vol. 401, no. 6755, pp. 788–791, 1999.
- [2] D. D. Lee, H. Sebastian, and S. y, "Algorithms for non-negative matrix factorization," in *Neural Information Processing Systems*, vol. 13, pp. 556–562, 2000.
- [3] F. Shahnaz, M. Berry, V. Pauca, and R. Plemmons, "Document clustering using nonnegative matrix factorization," *Information Processing & Management*, vol. 42, no. 2, pp. 373–386, 2006.
- [4] C. F. Yang, M. Ye, and J. Zhao, "Document clustering based on nonnegative sparse matrix factorization," in *International Conference on Computing, Networking and Communications*, 2005.
- [5] W. Wu, S. Kwong, Y. Zhou, Y. Jia, and W. Gao, "Nonnegative matrix factorization with mixed hypergraph regularization for community detection," *Information Sciences*, vol. 435, pp. 263–281, 2018.
- [6] Y.-X. Wang and Y.-J. Zhang, "Nonnegative matrix factorization: A comprehensive review," *IEEE Transactions on Knowledge and Data Engineering*, vol. 25, no. 6, pp. 1336–1353, 2013.
- [7] D. Kuang, S. Yun, and H. Park, "Symmmf: nonnegative low-rank approximation of a similarity matrix for graph clustering," *Journal of Global Optimization*, vol. 62, no. 3, pp. 545–574, 2015.
- [8] C. Ding, X. He, and H. D. Simon, "On the equivalence of nonnegative matrix factorization and spectral clustering," in *SDM* (H. Kargupta, J. Srivastava, C. Kamath, and A. Goodman, eds.), pp. 606–610, 2005.
- [9] B. Long, Z. Zhang, X. Wu, and P. S. Yu, "Relational clustering by symmetric convex coding," in *International Conference on Machine Learning*, 2007.
- [10] D. Kuang, H. Park, and C. Ding, "Symmetric nonnegative matrix factorization for graph clustering," in *SDM*, 2012.
- [11] W. Wu, Y. Jia, S. Kwong, and J. Hou, "Pairwise constraint propagation-induced symmetric nonnegative matrix factorization," *IEEE Transactions on Neural Networks and Learning Systems*, vol. 29, no. 12, pp. 6348–6361, 2018.
- [12] L. Zelnik-Manor and P. Perona, "Self-tuning spectral clustering," in *Neural Information Processing Systems*, 2004.
- [13] U. von Luxburg, "A tutorial on spectral clustering," *Statistics and Computing*, vol. 17, no. 4, pp. 395–416, 2007.
- [14] Y. Jia, H. Liu, J. Hou, and S. Kwong, "Semisupervised adaptive symmetric non-negative matrix factorization," *IEEE Transactions on Cybernetics*, vol. 51, no. 5, pp. 2550–2562, 2021.
- [15] F. Nie, X. Wang, and H. Huang, "Clustering and projected clustering with adaptive neighbors," *Proceedings of the 20th ACM SIGKDD international conference on Knowledge discovery and data mining*, pp. 977–986, 2014.
- [16] S. Huang, Z. Xu, and F. Wang, "Nonnegative matrix factorization with adaptive neighbors," *2017 International Joint Conference on Neural Networks (IJCNN)*, pp. 486–493, 2017.
- [17] Q. Wang, X. He, X. Jiang, and X. Li, "Robust bi-stochastic graph regularized matrix factorization for data clustering," *IEEE Transactions on Pattern Analysis and Machine Intelligence*, vol. 44, no. 1, pp. 390–403, 2022.
- [18] Y. Jia, H. Liu, J. Hou, and S. Kwong, "Clustering-aware graph construction: A joint learning perspective," *IEEE Transactions on Signal and Information Processing over Networks*, vol. 6, pp. 357–370, 2020.
- [19] Y. Jia, H. Liu, J. Hou, and S. Kwong, "Semisupervised adaptive symmetric non-negative matrix factorization," *IEEE Transactions on Cybernetics*, vol. 51, no. 5, pp. 2550–2562, 2021.
- [20] Y. Jia, H. Liu, J. Hou, and S. Kwong, "Pairwise constraint propagation with dual adversarial manifold regularization," *IEEE Transactions on Neural Networks and Learning Systems*, vol. 31, no. 12, pp. 5575–5587, 2020.
- [21] Y. Jia, J.-N. Li, W. Wu, and R. Wang, "Semi-supervised symmetric matrix factorization with low-rank tensor representation," *ArXiv*, vol. abs/2405.02688, 2024.
- [22] W. Wu, Y. Jia, S. Wang, R. Wang, H. Fan, and S. Kwong, "Positive and negative label-driven nonnegative matrix factorization," *IEEE Transactions on Circuits and Systems for Video Technology*, vol. 31, no. 7, pp. 2698–2710, 2021.
- [23] S. Paul and Y. Chen, "Orthogonal symmetric non-negative matrix factorization under the stochastic block model," *arXiv preprint arXiv:1605.05349*, 2016.
- [24] F. Pompili, N. Gillis, P. A. Absil, and F. Glineur, "Two algorithms for orthogonal nonnegative matrix factorization with application to clustering," *Neurocomputing*, vol. 141, no. SI, pp. 15–25, 2014.
- [25] C. Ding, T. Li, W. Peng, and H. Park, "Orthogonal nonnegative matrix t-factorizations for clustering," in *Knowledge Discovery and Data Mining*, 2006.
- [26] S. Wang, T.-H. Chang, Y. Cui, and J.-S. Pang, "Clustering by orthogonal nmf model and non-convex penalty optimization," *IEEE Transactions on Signal Processing*, vol. 69, pp. 5273–5288, 2021.
- [27] B. Li, G. Zhou, and A. Cichocki, "Two efficient algorithms for approximately orthogonal nonnegative matrix factorization," *IEEE Signal Processing Letters*, vol. 22, no. 7, pp. 843–846, 2015.
- [28] T. Liu, M. Gong, and D. Tao, "Large-cone nonnegative matrix factorization," *IEEE Transactions on Neural Networks and Learning Systems*, vol. 28, no. 9, pp. 2129–2142, 2017.
- [29] L. Hou, D. Chu, and L.-Z. Liao, "A progressive hierarchical alternating least squares method for symmetric nonnegative matrix factorization," *IEEE Transactions on Pattern Analysis and Machine Intelligence*, vol. 45, no. 5, pp. 5355–5369, 2023.
- [30] Y. Jia, H. Liu, J. Hou, S. Kwong, and Q. Zhang, "Self-supervised symmetric nonnegative matrix factorization," *IEEE Transactions on Circuits and Systems for Video Technology*, vol. 32, no. 7, pp. 4526–4537, 2022.
- [31] W. Li, J. Li, X. Liu, and L. Dong, "Two fast vector-wise update algorithms for orthogonal nonnegative matrix factorization with sparsity constraint," *J. Comput. Appl. Math.*, vol. 375, p. 112785, 2020.
- [32] A. Ng, M. Jordan, and Y. Weiss, "On spectral clustering: Analysis and an algorithm," in *Neural Information Processing Systems* (T. Dietterich, S. Becker, and Z. Ghahramani, eds.), vol. 14, pp. 849–856, 2002.
- [33] W. Wang and M. Á. Carreira-Perpiñán, "Projection onto the probability simplex: An efficient algorithm with a simple proof, and an application," *ArXiv*, vol. abs/1309.1541, 2013.
- [34] V. Vasudevan and M. Ramakrishna, "A hierarchical singular value decomposition algorithm for low rank matrices," *ArXiv*, vol. abs/1710.02812, 2017.
- [35] Z. Zhu, X. Li, K. Liu, and Q. Li, "Dropping symmetry for fast symmetric nonnegative matrix factorization," in *Neural Information Processing Systems* (S. Bengio, H. Wallach, H. Larochelle, K. Grauman, N. CesaBianchi, and R. Garnett, eds.), vol. 31, 2018.
- [36] Q. Shi, H. Sun, S. Lu, M. Hong, and M. Razaviyayn, "Inexact block coordinate descent methods for symmetric nonnegative matrix factorization," *IEEE Transactions on Signal Processing*, vol. 65, no. 22, pp. 5995–6008, 2017.
- [37] Z. Gao, N. Guan, and L. Su, "Graph regularized symmetric non-negative matrix factorization for graph clustering," *2018 IEEE International Conference on Data Mining Workshops (ICDMW)*, pp. 379–384, 2018.